NMR evidence for the partially gapped state in $CeOs_2Al_{10}$

C. S. Lue,[1,*] S. H. Yang,[1] T. H. Su,[1] and Ben-Li Young[2]
[1]*Department of Physics, National Cheng Kung University, Tainan 70101, Taiwan*
[2]*Department of Electrophysics, National Chiao Tung University, Hsinchu 30010, Taiwan*
(Received 9 September 2010; published 22 November 2010)

We report the results of a ^{27}Al nuclear magnetic resonance (NMR) study of $CeOs_2Al_{10}$ at temperatures between 4 and 300 K. This material has been of current interest due to indications of hybridization gap behavior below the transition temperature $T_o \simeq 29$ K. Five ^{27}Al NMR resonance lines that are associated with five nonequivalent crystallographic aluminum sites have been resolved. For each individual aluminum site, the low-temperature NMR Knight shift goes over a thermally activated response. The temperature-dependent spin-lattice-relaxation rate exhibits a rapid drop below T_o, indicative of the formation of an energy gap in this material. We interpret the Knight shift and the relaxation-rate data in light of the presence of a pseudogap with residual electronic density of states at the Fermi level. Moreover, the magnitude of the pseudogap of 120 K is extracted from NMR results, in agreement with the value obtained from the inelastic neutron-scattering experiment.

DOI: 10.1103/PhysRevB.82.195129 PACS number(s): 75.30.Mb, 76.60.−k

I. INTRODUCTION

The recently discovered $YbFe_2Al_{10}$-type $CeOs_2Al_{10}$ intermetallic has attracted lots of interest because of the anomalous temperature dependence of its various physical properties.[1,2] The electrical resistivity ρ exhibits semiconducting behavior at high temperatures and follows a metal-insulator phase transition at $T_o \simeq 29$ K. Below about 15 K, ρ raises again with decreasing temperature, commonly observed in a semiconductor or a semimetal. The phase transition feature is suppressed under an external pressure of about 2 GPa and the insulating character disappears with a metallic response in ρ.[1] Associated with this phase transition, the magnetic susceptibility (χ) and heat capacity (C_p) show clear thermally activated behavior below T_o. These observations indicated that the phase transition may be accounted for by the formation of an energy gap over a portion of the Fermi surfaces.[1,2]

In this regard, it is important to provide evidence for the existence of a gapped state in $CeOs_2Al_{10}$ and examine whether this material follows semiconducting or semimetal physics. Nuclear magnetic resonance (NMR) is a local probe yielding information about Fermi-surface features below the transition temperature. The NMR temperature dependence allows us to characterize the intrinsic properties of $CeOs_2Al_{10}$. In this paper, we present NMR measurements including ^{27}Al powder patterns, Knight shifts, as well as spin-lattice-relaxation rates in $CeOs_2Al_{10}$ at temperatures between 3.8 and 300 K. The NMR results reveal an energy gap of about 120 K but with residual density of states (DOS) at the Fermi level in this compound. Thus, we provide the microscopic confirmation that the observed gap in $CeOs_2Al_{10}$ is actually a pseudogap with finite charge carriers in the Fermi-level DOS.

II. EXPERIMENT AND DISCUSSION

Polycrystalline $CeOs_2Al_{10}$ was prepared by an ordinary arc-melting technique. Briefly, the mixture of 99.9% Ce, 99.99% Os, and 99.99% Al elemental metals with the stoichiometric ratio was placed in a water-cooled copper hearth and then melted several times in an argon-flow arc melter. The weight loss during melting is less than 0.5%. To promote homogeneity, the as-cast sample was annealed in a vacuum-sealed quartz tube at 800 °C for three days, followed by furnace cooling. A room-temperature x-ray diffraction taken with Cu $K\alpha$ radiation on the powder specimen was identified within the expected $YbFe_2Al_{10}$-type structure (*Cmcm* phase).[3]

NMR measurements were performed under a constant field of 6.9437 T. A home-built probe was employed for both room-temperature and low-temperature experiments. To avoid the skin depth problem of the rf transmission power, a powder sample was used. The specimen was put in a plastic vial that showed no observable ^{27}Al NMR signal.

A. Powder patterns

Based on the atomic-positional parameters of the $YbFe_2Al_{10}$-type structure,[3] aluminum atoms have five nonequivalent crystallographic sites in $CeOs_2Al_{10}$. In order to explore the local electronic properties for each Al site, we carried out nuclear quadrupole resonance measurements providing well-resolved satellite lines for all Al sites. In this investigation, wide-line satellite spectra were mapped out by integrating spin-echo signals of various excitations. Due to electric quadrupole coupling, the ^{27}Al NMR spectra ($I=\frac{5}{2}$) are composed of five transition lines per site so that five nonequivalent Al sites result in 25 resonance lines. In addition to the central transition lines which were displayed separately in Fig. 2, the remaining 20 satellite lines were resolved, as demonstrated in Fig. 1. The sharp satellite line feature in $CeOs_2Al_{10}$ indicates that this material is well ordered, as the disorder effect usually broadens the NMR spectrum due to hyperfine-field inhomogeneity.[4]

For a powder sample, as in our experiment, these lines exhibit a typical powder pattern, with distinctive edge features corresponding to the quadrupole parameters. The four-

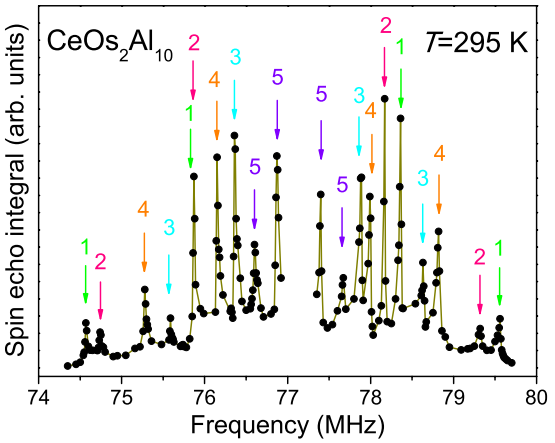

FIG. 1. (Color online) Room-temperature ^{27}Al NMR satellite lines for five nonequivalent crystallographic Al sites in $CeOs_2Al_{10}$.

edge singularities for each Al site arise from $m=\pm\frac{1}{2}\leftrightarrow\pm\frac{3}{2}$ and $m=\pm\frac{3}{2}\leftrightarrow\pm\frac{5}{2}$ transitions. Although all Al sites in $CeOs_2Al_{10}$ are nonaxial in the crystallographic environment, we found nearly even separation of the satellite lines for each individual site. It indicates that the corresponding asymmetric parameter η is very small, estimated to be less than 0.05 within the accuracy of the peak positions. Therefore, it is valid to determine the quadrupole frequency, ν_Q, directly from the splitting of these lines because the first-order quadrupole interaction is the main effect shaping the satellite lines. Here $\nu_Q=3eQV_{zz}/2I(2I-1)h$ is defined by the nuclear quadrupole moment Q and the largest principal axis component of the electric field gradient (EFG) tensor V_{zz}.

Site identification for $CeOs_2Al_{10}$ is given by analogy to the isostructural $YbFe_2Al_{10}$-type compounds based on the site-symmetry criteria as follows.[3,5–8] Each Al(5) atom occupies the 8*e* site which is the highest atomic-site symmetry among these five Al sites. Therefore Al(5) experiences the weakest EFG from the surrounding neighbors, corresponding to the smallest ν_Q of 0.54 MHz for this site. Al(1) and Al(2) have the same site symmetry, 8*g*, the lowest point symmetry in the present crystallographic environment. Also the averaged interatomic distance of the surrounding atoms measured from Al(1) is shorter than that from Al(2), leading to the strongest EFG sensed by the Al(1) site. It is thus reasonable to associate the largest ν_Q of 2.5 MHz with this site. The Al(3) and Al(4) atoms reside the 8*f* sites and Al(3) has a longer averaged interatomic distance than that of Al(4). By analogy to the comparison between Al(1) and Al(2), a relative small ν_Q of 1.53 MHz should be assigned to the Al(3) site. On these bases, all observed satellite lines for $CeOs_2Al_{10}$ were thus indexed and the corresponding ν_Q values were summarized in Table I.

It is noticeable that we have employed the same argument for the Al-site assignment in the isostructural $CeFe_2Al_{10}$ and $CeRu_2Al_{10}$,[8,9] yielding a consistent trend for the ν_Q values among these systems. Matsumura an co-workers have carried out ^{27}Al nuclear quadrupole resonance measurements on both materials using different Al-site identification.[10,11] In spite of this discrepancy, part of ν_Q values were found to be identical with ours. Also the important physical properties

TABLE I. Asymmetry parameter η, quadrupole frequency ν_Q in MHz, temperature-independent Knight shift $K(0)$ in %, and hyperfine coupling constant A_{hf} in kOe/μ_B for each individual Al site of $CeOs_2Al_{10}$.

Site	η	ν_Q	$K(0)$	A_{hf}
Al(1)	≤0.05	2.50	0.15	3.08
Al(2)	≤0.05	2.30	0.05	1.33
Al(3)	≤0.05	1.53	0.34	5.19
Al(4)	≤0.05	1.65	0.09	1.94
Al(5)	≤0.05	0.54	0.40	6.85

such as the pseudogap features were in agreement with each other. It thus points out that the difference in the site assignment has no influence on the present observation of the partially gapped state in $CeOs_2Al_{10}$.

Central transition ($m=+\frac{1}{2}\leftrightarrow-\frac{1}{2}$) line shapes were obtained from spin-echo fast Fourier transforms using a standard $\pi/2$-τ-π sequence. Several representative spectra taken at various temperatures were showed in Fig. 2. As one can see, these spectra are quite complicated because of the combination of five Al sites. Attempts to decompose each spectrum into five components using quadruple broadening together with the anisotropic Knight shift effect cannot yield an unambiguous result. On the other hand, we can resolve each Al site from quadrupole transitions as the central transition line appears approximately at the midpoint of the separated satellite lines. With this respect, we denoted five central transition lines from the high-frequency side as Al(5), Al(3), Al(1), Al(4), and Al(2), respectively. Such a result indicates that Al(5) and Al (3) have large Knight shifts relative to other Al sites. This result is quite reasonable because both sites

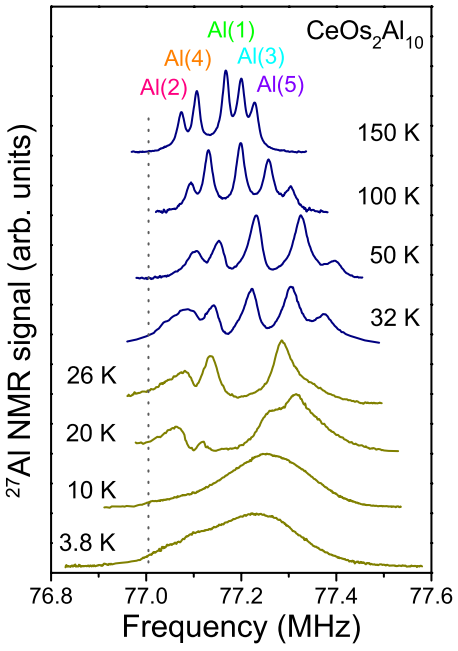

FIG. 2. (Color online) ^{27}Al NMR central transition spectra of $CeOs_2Al_{10}$ measured at various temperatures. The dashed vertical line denotes the position of the ^{27}Al reference frequency.

contain two Ce atoms among their near neighbors,[5,6] and thus experience strong transferred hyperfine coupling from Ce spins.

At high temperatures, ^{27}Al NMR spectra exhibit a clear five-line feature with relative narrow linewidth for each line. The linewidth gradually increases with lowering temperature due to an increase in magnetic dipolar interactions upon cooling. Below T_o, the feature of the line splitting smears out and the corresponding spectrum exhibits a three-peak feature. The low-frequency part is dominated by Al(2), Al(4), and Al(1) sites while the high-frequency potion would be the combination of Al(3) and Al(5) sites. With further decreasing temperature, all transition lines merge together, resulting in a single broad spectrum spreading within a frequency range of about 400 kHz. It is known that the width of the NMR spectrum reflects the nature of magnetic interactions, providing a direct identification for the presence of magnetic ordering.[12] To estimate the linewidth of each Al site, we decomposed the spectrum into five Gaussian functions, yielding an upper limit for the linewidth of $\simeq$60 kHz at 3.8 K. This value is only about three times larger than those measured at a room temperature, indicative of a moderate line broadening in the ground state. Such a result implies a very small or zero internal field accompanied by magnetic ordering if the transition is driven by the magnetic origin. This finding is consistent with a recent zero-field μ^+SR experimental result, revealing a weak internal field of about 20 G with another component of 50 G.[13] Also the observation of a small internal field is reminiscent of that found in its Ru analog which develops an internal field of 30 G below the transition temperature of 27 K.[14,15] According to the comparison, it reinforces the conclusion that $CeOs_2Al_{10}$ and $CeRu_2Al_{10}$ possess common characteristics of the phase transition as well as the magnetic features.

B. Knight shifts

The observed T-dependent ^{27}Al NMR Knight shifts (K_{obs}'s) for all Al sites of $CeOs_2Al_{10}$ were displayed in Fig. 3. Here K_{obs} was estimated from the center of the gravity of the corresponding central transition line, referred to the ^{27}Al resonance frequency of one molar aqueous $AlCl_3$. It is apparent that the high-temperature variation in each K_{obs} is consistent with the magnetic susceptibility χ, showing a broad maximum at around $T_{max}\simeq 45$ K. In general, each K_{obs} here is related to χ by the expression

$$K_{obs}^{(i)}(T) = K_o^{(i)} + \frac{A_{hf}^{(i)}}{N_A\mu_B}\chi(T), \quad i = 1-5. \tag{1}$$

Here $A_{hf}^{(i)}$ is the hyperfine coupling constant due to an intermixing of Al s and Ce f states for the specific Al site. The data of χ here were measured with a superconducting quantum interference device magnetometer (Quantum Design) under an external field of 1 T. The temperature dependence of $\chi(T)$ in the range between 2 and 300 K was given in the inset of Fig. 4. The Clogston-Jaccarino plot, showing the observed Knight shifts against χ, is given in Fig. 4. Each linear behavior demonstrates a unique hyperfine coupling constant and the slope yields a value of $A_{hf}^{(i)}$ for the corresponding Al site. The magnitudes of $A_{hf}^{(i)}$ ranging from 1.33 to 6.85 kOe/μ_B were obtained with the results listed in Table I.

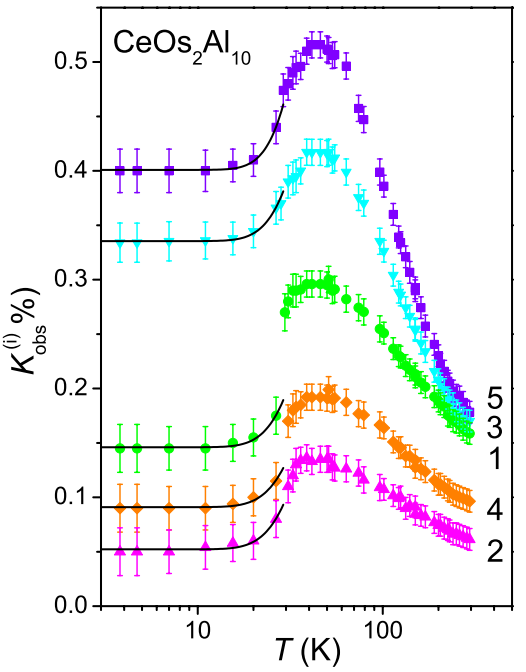

FIG. 3. (Color online) Temperature dependence of observed ^{27}Al NMR Knight shifts in $CeOs_2Al_{10}$. Solid curves: fits to the thermally activated form described in the text.

Below T_o, all K_{obs}'s exhibit thermally activated behavior, indicative of a gap feature in the energy spectrum. Here, each low-T Knight shift follows $K(T)=K(0)+C_o\exp(-\Delta_K/T)$.

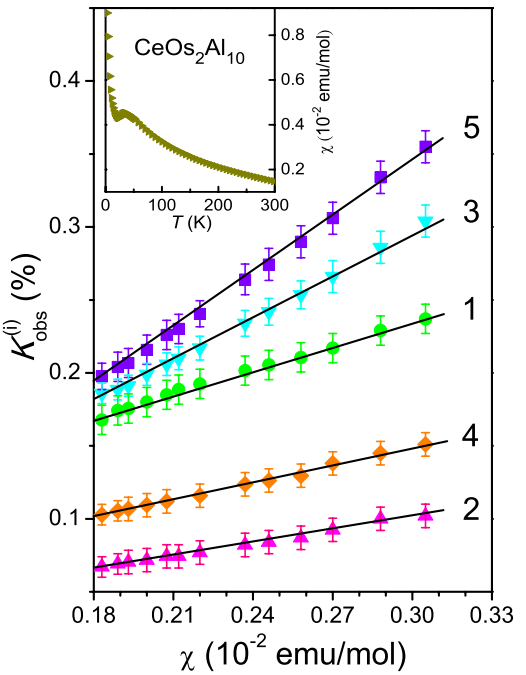

FIG. 4. (Color online) Variation in the observed Knight shifts versus the magnetic susceptibility in $CeOs_2Al_{10}$. Each solid line indicates the linear relationship. Inset: measured bulk magnetic susceptibility of $CeOs_2Al_{10}$ under a constant field of 1 T.

The first term $K(0)$ represents the T-independent Knight shift as extrapolating to $T=0$ and the second is a thermally activated form characterized by an energy gap Δ_K. Each least-square fit, shown as a solid curve, gives $\Delta_K=115\pm15$ K. This estimate is consistent with the specific heat and χ results extracted from the measurements on single-crystal samples.[1,2]

We found that the magnitudes of $K(0)$ for $CeOs_2Al_{10}$ are quite large and this result disagrees with the expectation for a material with a true energy gap. For a semiconductor, there is no residual DOS at the Fermi level and the corresponding T-independent Knight shift would be attributed to the orbital shift (K_{orb}). Comparing to other ^{27}Al NMR shifts in solids,[16] for example, the zinc-blende semiconductors with shifts in the range +0.007–+0.014 %, we see that several $K(0)$'s here are unreasonable large, very unlikely to be accounted for by the orbital shift only. Rather, the s-contact Knight shift (K_s) should contribute to the observed shift for the present case of $CeOs_2Al_{10}$. This implies that there exists a finite number of charge carriers at the Fermi surfaces according to the relationship of the s-contact Knight shift to the s-DOS in metals.[17] With this respect, the scenario of a pseudogap rather than a band gap would be more realistic to the understanding of the band feature around the Fermi level of $CeOs_2Al_{10}$. Such an argument is consistent with the low-T specific-heat data,[2] showing a moderate linear specific-heat coefficient $\gamma=10$ mJ/mol K^2, which seems too large for a real semiconductor. A similar observation was found for CeIrSb, which was originally considered to possess a true gap, but found from the Knight shift analysis to be a semimetal with a narrow pseudogap at the Fermi level.[18]

C. Spin-lattice-relaxation rates

To gain more insight into the gap or pseudogap feature of $CeOs_2Al_{10}$, we carried out the spin-lattice-relaxation rate $(1/T_1)$ measurement, being sensitive to the low-energy excitations. Because it is difficult to isolate these central lines in the relaxation-rate experiment, we only measured the high-frequency line, mainly associated with the Al(5) site. The temperature variation in $1/T_1$ of $CeOs_2Al_{10}$ was illustrated in Fig. 5. The result of $1/T_1$ clearly shows evidence for the rapid drop below T_o, a signature of gap behavior. With a close view of the $1/T_1$ feature, we found that $1/T_1$ is nearly proportional to the temperature below about 10 K, as presented in the inset of Fig. 5. Therefore, the obtained low $T1/T_1$ can be expressed as $1/T_1=C_1T+C_2\exp(-\Delta_R/T)$. Here, the first term represents a constant $1/T_1T$ which is due to the Korringa process, associated with the relaxation of s-character electrons. The second is characterized by an energy gap Δ_R, similar to the thermally activated form in the Knight shift. Accordingly, a fit to the above equation using C_1, C_2, and Δ_R as parameters was performed. As shown in the inset of Fig. 5, the fit is quite satisfactory, yielding $C_1=0.12\pm0.02$ s^{-1} K^{-1}, $C_2=180\pm10$ s^{-1}, and $\Delta_R=120\pm20$ K. Remarkably, the deduced gap of about 120 K is almost identical with the 11 meV (128 K) peak revealed in the inelastic neutron-scattering experiment,[13] pointing to the same energy excitation probed by both measurements. It

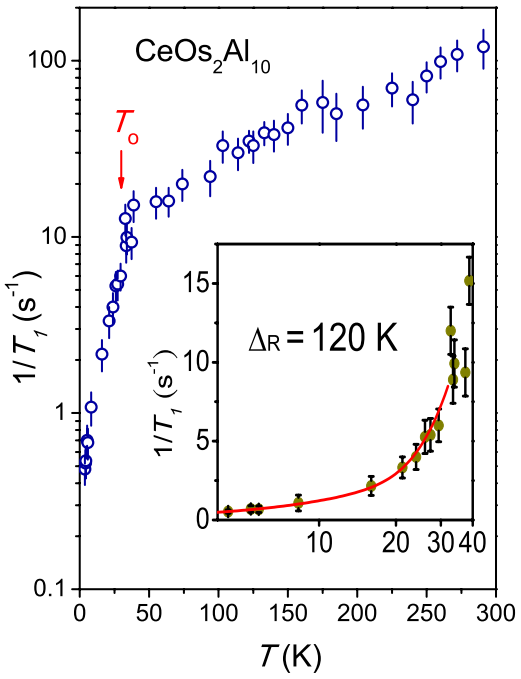

FIG. 5. (Color online) Temperature dependence of ^{27}Al spin-lattice-relaxation rates in $CeOs_2Al_{10}$. The arrow indicates the phase transition temperature. The inset shows the low-T relaxation rates which are fitted to the Korringa term plus activated behavior.

is worthwhile mentioning that the gap size obtained in $CeOs_2Al_{10}$ is a bit larger than its isostructural compound $CeRu_2Al_{10}$ which also exhibits gapped behavior with $\Delta\simeq100$ K below the transition temperature.[1,2,9,19]

From the analysis of relaxation rates, we found a nonzero term of C_1 which clearly demonstrates the non-negligible Korringa behavior in $CeOs_2Al_{10}$, indicative of finite charge-carrier density at the Fermi level. It should be noted that trying to omit the Korringa constant by fixing $C_1=0$ cannot reproduce the low-$T1/T_1$ data of this material. Our NMR investigation thus strongly supports the picture of the existence of a pseudogap in $CeOs_2Al_{10}$ below T_o. Similar features have been reported in several Kondo systems such as CeIrSb, CeNiSn, U_2Ru_2Sn, and $CeRu_4Sn_6$,[18,20–22] which were finally characterized as semimetals with the Fermi levels located in the pseudogaps. Furthermore, the deduced gap size of 120 K in $CeOs_2Al_{10}$ is typical of hybridization-driven gap in other rare-earth intermetallic systems. With these respects, the present NMR observations allow us to add $CeOs_2Al_{10}$ to the category of hybridized pseudogap systems.

III. CONCLUSIONS

In conclusion, the ^{27}Al NMR investigation indicates that an energy gap opens partially on the Fermi surface of $CeOs_2Al_{10}$ associated with the phase transition at $T_o\simeq29$ K. The analyses of the Knight shift as well as the relaxation rate confirm that the observed gapped behavior is not actually a real gap but rather a pseudogap. The

pseudogap characteristics of $CeOs_2Al_{10}$ are similar to other semimetallic Ce-based Kondo systems such as CeNiSn, $CeRu_4Sn_6$, and CeRhSb,[20,22–24] which were believed to be formed by strong hybridization between localized $4f$ electrons and conduction electrons. In addition, the narrow pseudogap of about 120 K extracted from the present NMR results is quite consistent with the values obtained from the bulk properties as well as the inelastic neutron-scattering measurements.

ACKNOWLEDGMENTS

This work was supported by the National Science Council of Taiwan under Grant No. NSC-98-2112-M-006-011-MY3 (C.S.L.).

*cslue@mail.ncku.edu.tw

[1] T. Nishioka, Y. Kawamura, T. Takesaka, R. Kobayashi, H. Kato, M. Matsumura, K. Kodama, K. Matsubayashi, and Y. Uwatoko, J. Phys. Soc. Jpn. **78**, 123705 (2009).
[2] Y. Muro, J. Kajino, K. Umeo, K. Nishimoto, R. Tamura, and T. Takabatake, Phys. Rev. B **81**, 214401 (2010).
[3] V. M. T. Thiede, T. Ebel, and W. Jeitschko, J. Mater. Chem. **8**, 125 (1998).
[4] C. S. Lue, T. H. Su, B. X. Xie, S. K. Chen, J. L. MacManus-Driscoll, Y. K. Kuo, and H. D. Yang, Phys. Rev. B **73**, 214505 (2006).
[5] H. Noël, A. P. Gonçalves, and J. C. Waerenborgh, Intermetallics **12**, 189 (2004).
[6] A. I. Tursina, S. N. Nesterenko, E. V. Murashova, I. V. Chernyshev, H. Noel, and Y. D. Seropegin, Acta Crystallogr., Sect. E: Struct. Rep. Online **61**, i12 (2005).
[7] Y. Muro, K. Motoya, Y. Saiga, and T. Takabatake, J. Phys. Soc. Jpn. **78**, 083707 (2009).
[8] S. C. Chen and C. S. Lue, Phys. Rev. B **81**, 075113 (2010).
[9] C. S. Lue, S. H. Yang, A. Abhyankar, Y. D. Hsu, H. T. Hong, and Y. K. Kuo, Phys. Rev. B **82**, 045111 (2010).
[10] M. Matsumura, Y. Kawamura, S. Edamoto, T. Takesaka, H. Kato, T. Nishioka, Y. Tokunaga, S. Kambe, and H. Yasuoka, J. Phys. Soc. Jpn. **78**, 123713 (2009).
[11] Y. Kawamura, S. Edamoto, T. Takesaka, T. Nishioka, H. Kato, M. Matsumura, Y. Tokunaga, S. Kambe, and H. Yasuoka, J. Phys. Soc. Jpn. **79**, 103701 (2010).
[12] C. N. Kuo, C. S. Lue, Z. He, and M. Itoh, Solid State Commun. **149**, 341 (2009).
[13] D. T. Adroja, A. D. Hillier, P. P. Deen, A. M. Strydom, Y. Muro, J. Kajino, W. A. Kockelmann, T. Takabatake, V. K. Anand, J. R. Stewart, and J. Taylor, Phys. Rev. B **82**, 104405 (2010).
[14] S. Kambe, H. Chudo, Y. Tokunaga, T. Koyama, H. Sakai, T. U. Ito, K. Ninomiya, W. Higemoto, T. Takesaka, T. Nishioka, and Y. Miyake, J. Phys. Soc. Jpn. **79**, 053708 (2010).
[15] D. D. Khalyavin, A. D. Hillier, D. T. Adroja, A. M. Strydom, P. Manuel, L. C. Chapon, P. Peratheepan, K. Knight, P. Deen, C. Ritter, Y. Muro, and T. Takabatake, Phys. Rev. B **82**, 100405(R) (2010).
[16] R. E. J. Sears, Phys. Rev. B **22**, 1135 (1980).
[17] C. S. Lue, S. Y. Wang, and C. P. Fang, Phys. Rev. B **75**, 235111 (2007).
[18] Y. Kawasaki, M. Izumi, Y. Kishimoto, T. Ohno, H. Tou, Y. Inaoka, M. Sera, K. Shigetoh, and T. Takabatake, Phys. Rev. B **75**, 094410 (2007).
[19] J. Robert, J.-M. Mignot, G. Andre, T. Nishioka, R. Kobayashi, M. Matsumura, H. Tanida, D. Tanaka, and M. Sera, Phys. Rev. B **82**, 100404(R) (2010).
[20] K.-i. Nakamura, Y. Kitaoka, K. Asayama, T. Takabatake, G. Nakamoto, H. Tanaka, and H. Fujii, Phys. Rev. B **53**, 6385 (1996).
[21] A. K. Rajarajan, A. Rabis, M. Baenitz, A. A. Gippius, E. N. Morozowa, J. A. Mydosh, and F. Steglich, Phys. Rev. B **76**, 024424 (2007).
[22] E. M. Brüning, M. Brando, M. Baenitz, A. Bentien, A. M. Strydom, R. E. Walstedt, and F. Steglich, Phys. Rev. B **82**, 125115 (2010).
[23] S. K. Malik and D. T. Adroja, Phys. Rev. B **43**, 6277 (1991).
[24] K. Nakamura, Y. Kitaoka, K. Asayama, T. Takabatake, H. Tanaka, and H. Fujii, J. Phys. Soc. Jpn. **63**, 433 (1994).